Dynamic Adaptive Robust Backstepping Control Design for an Uncertain Linear System

Hadi Hajieghrary
Graduate Research Assistant
Scalable Autonomous Systems Lab
Drexel University
Philadelphia, PA 19104
Email: Hadi.Hajieghrary@drexel.edu

M. Ani Hsieh
Associate Professor
Scalable Autonomous Systems Lab
Drexel University
Philadelphia, PA 19104
Email: MHsieh1@drexel.edu

This paper builds on the existing adaptive robust control (ARC) synthesis method introduced by Yao et al. and presents a new method to synthesize adaptive robust controllers. Based on dynamic backstepping, the approach explicitly addresses the uncertain dynamics which enters into the system via the higher order channels of the state space model. As such, the proposed D-ARC method addresses the inherent weakness of the original approach where uncertainty in the higher order channels are ignored. The proposed approach is illustrated in simulations for controlling a voice coil motor (VCM) actuator that serves as a read/write head for a single stage hard disk drive (HDD). The effectiveness of the resulting D-ARC controller is validated by considering the transient performance, tracking errors, and disturbance rejection of the VCM operating in both the track seeking and track following modes.

1 Introduction

Existing efforts in synthesizing suitable controllers for systems that exhibit uncertain nonlinear dynamics generally fall into two categories: adaptive control (AC) and deterministic robust control (DRC). AC approaches are generally better at dealing with structured or parametric uncertainties but conventional strategies can suffer from poor parameter estimation leading to unpredictable system performance. These drawbacks are more pronounce when the system is subject to uncertainties resulting from unmodeled dynamics and output disturbances [1]. In contrast, DRC strategies are capable of dealing with both dynamic and parametric uncertainties. In addition, systems with robust feedback can reach predetermined, rather than zero, steady-state errors. However, to decrease the steady-state error, the robust controller would often have to exert significant control effort, possibly at undesirably high levels.

To address these drawbacks, Yao *et al.* introduced adaptive robust control (ARC) which combines the strengths of both adaptive and robust control approaches [2]. The ARC is a feedback strategy that can guarantee the stability of a system regardless of the type of disturbances and unmodeled dynamics. The robust part of the controller exploits the adaptive part of the controller to decrease the tracking error at the steady state [3]. The result is a system that benefits from both adaptive and the robust control by targeting the different performance regimes of the system that each is best at impacting. By coordinating the adaptive and robust feedback features, ARC enables robust performance of the system in the low frequency domain in the presence of model parameter uncertainties. The adaptive component of the controller allows the system to better track the desired reference trajectory without the need for excessive control effort. Simultaneously, in the high frequency regime where the system is prone to disturbances resulting from unmodeled dynamics, the robust component of the controller can guarantee the stability of the system.

To address the problem of ARC design, Yao *et al.* presented an innovative approach to model both the parametric and dynamic uncertainties of the system within a systematic backstepping framework [4]. However, the proposed modeling approach cannot be easily handled using conventional backstepping design methods since the backstepping procedure stops once it encounters the input signal in the design process, leaving the parametric and dynamic uncertainty terms in the model untouched. Yet, the procedure is often used in ARC design which often results in poor closed-loop performance, or worse, instability. An alternative synthesis approach for dynamical backstepping design was proposed by Zinober et al [5]. In this work, the design methodology does not stop when it encounters the control signal but rather encapsulates as many system states as it can into a Lyapunov function. The advantages of this approach include the accounting of all the uncertainty model structure in the design of the robust controller as well as the inclusion of the control input in the design of the Lyapunov function. The result is smoother system performance when controller is in place.

In this work, we build upon [5] to extend Yao *et al.*'s [2] design method to target the uncertainties not impacted by the original ARC design. The novelty of the contribution lies in how the proposed control synthesis algorithm handles the uncertainties in the system model and the disturbances the system is subject to. In the original ARC design, Yao *et al.* modeled these uncertainties as disturbance signals fed to each dynamic channel of the system. The original procedure then considers each channel individually by identifying the unknown parameters of the model and proportionally strengthening the robust design. However, the conventional backstepping design procedure is incomplete since it stops after the actual control variable is obtained, failing to properly address the remaining uncertainties. We present a modification to Zinober *et al.*'s procedure to improve the ARC design.

To illustrate and evaluate the proposed design methodology, we synthesize a feedback control strategy for a voice coil motor (VCM) which is used as a precision motion actuator in a hard disk drive (HDD). The VCM actuates the read/write head in a HDD and must be able to transition quickly from one track to another when it is operating in "track-seeking" mode. The VCM must also precisely land the read/write head on and enable it to follow the right target track when it operates in the "track-following" mode. We employ an ARC to enable the VCM to achieve these precise maneuvers. The system identification data set of the HDD servo system, including the VCM, is provided by Postlethwaite *et al.* [6]. While the nominal system fitted for data in [6] is a non-minimum phase system, the VCM is actually a minimum phase system, especially when the sensor and actuator are none-collocated [7]. The difference arise from the flexibility of the arm which contributes a limiting non-minimum phase zero into the overall transfer function [8]. The non-minimum phase zeros of the nominal linear system becomes the internal dynamics of the closed-loop system when the feedback controller is designed using the backstepping technique which destabilizes the system internally [9]. In this paper, the nominal higher order system is reduced to a minimum phase lower order one. We show that our approach results in a controller that is can stabilize the unstable internal dynamics of the system despite using a backstepping design procedure.

The rest of paper is organized as follows: Section 2 formally states the problem, Section 3 describes the control design methodology, Section 4 presents the simulation results, and Section 5 concludes the paper with a discussion on the effectiveness of the proposed method.

2 Problem statement

Consider a single input-single output (SISO) system described using the mixed notation given by

$$y(t) = \frac{B(s)}{A(s)}u(t) + \frac{D(s)}{A(s)}\Lambda(t) + \delta_y(t), \tag{1}$$

where $A(s) = s^n + a_{n-1}s^{n-1} + \cdots + a_1 s + a_0$, $B(s) = b_m s^m + b_{m-1}s^{m-1} + \cdots + b_1 s + b_0$, and $D(s) = d_l s^l + d_{l-1}s^{l-1} + \cdots + d_1 s + d_0$. The system is strictly proper, *i.e.*, $n > l, m$. The parameters a_i and b_i are unknown constants while d_i is assumed to be known. The transfer function $\frac{D(s)}{A(s)}$ determines the frequency bound on which the internal disturbances distort the output of the system. All the results can be extended to the case when the d_i parameters are unknown.

If the model of the system is fairly accurate and the only concern is the unstructured disturbances, all the uncertainty of the system can be modeled as a lumped unstructured output uncertainty. However, the current model helps us extract the constituent parts of the disturbances, which is mainly the result of structural deficiencies in the modeling, and design an estimator to identify it. As shown in Eqn. (1) the auxiliary input variable $\Lambda(t)$ represents the dynamic disturbance coming from the intermediate channels of the plant with $\delta_y(t)$ the output disturbance. This dynamic uncertainty is modeled as [2] $\Lambda(t) = Q^T\Sigma + \Delta(t)$. We can represent the disturbance as a linear combination of *known* basis functions, $Q(t) = [q_p(t), q_{p-1}(t), \ldots, q_1(t)]^T$, and *unknown* constant coefficients, $\Sigma = [\sigma_p, \sigma_{p-1}, ..., \sigma_1]^T$. This represents the core of the dynamic uncertainty which we will explicitly use in the controller design to maintain stability and improve the system's achievable performance. Additionally, $\Delta(t)$ is the disturbance modeling error which we will deal with by modifying the robust control action to achieve robust performance. Given this disturbance model, the plant given by Eqn. (1) is represented in state space form as follows:

$$\begin{aligned}
\dot{x}_1 &= x_2 - a_{n-1}x_1 \\
&\vdots \\
\dot{x}_{n-l} &= x_{n-l+1} - a_l x_1 + d_l Q^T\Sigma + d_l\Delta \\
&\vdots \\
\dot{x}_\rho &= x_{\rho+1} - a_m x_1 + d_m Q^T\Sigma + d_m\Delta + b_m u \\
&\vdots \\
\dot{x}_n &= -a_0 x_1 + d_0 Q^T\Sigma + d_0\Delta + b_0 u \\
y &= x_1 + \delta_y(t),
\end{aligned} \tag{2}$$

where $\rho = n - m$ is the relative degree of the system, and without loss of generality it is assumed that $m < l$. Figure 1 gives the block diagram for the system described by Egn. (2). We make the following assumptions in regards to the system and the uncertainties the system is subject to:

Assumption 1: Nominal plant is minimum phase.
Assumption 2: The sign of b_m is known.
Assumption 3: The extent of parametric uncertainties, $\Theta \stackrel{\text{def}}{=} [-a_{n-1}, \ldots, -a_0, b_m, \ldots, b_0, \sigma_p, \ldots, \sigma_1]$ and the upper bound on uncertain nonlinearities are known, *i.e.*, $\Theta \in \Omega_\Theta \triangleq \{\Theta | \Theta_{min} < \Theta < \Theta_{max}\}$, $\Delta \in \Omega_\Delta \triangleq \{\Delta(t) | \|\Delta(t)\| < \delta_y\}$, $\delta_y(t) \in \Omega_d \triangleq \{\delta_y(t) | \|\delta_y(t)\| < \delta_d\}$, and $\dot{\delta}_y(t) \in \Omega_f \triangleq \{\dot{\delta}_y(t) | \|\dot{\delta}_y(t)\| < \delta_f\}$.

As such, given the reference trajectory, $y_r(t)$, the objective of the design is to synthesize a control signal, $u(t)$, such

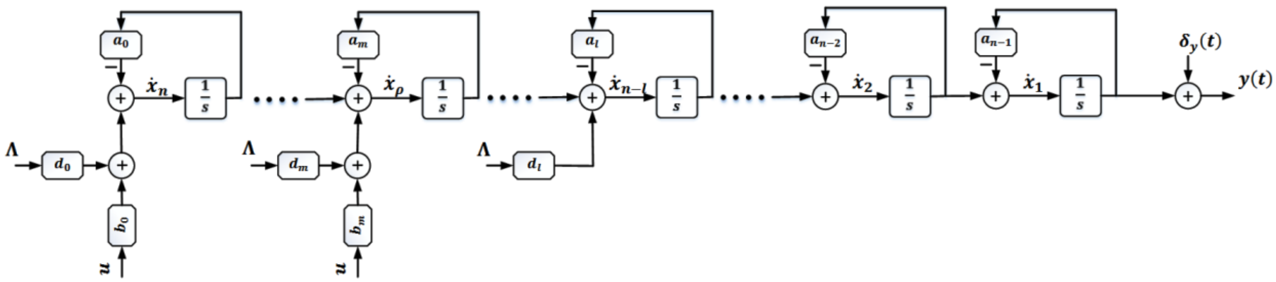

Fig. 1. The overall schematic of the linear uncertain system.

that the output, $y(t)$, tracks the reference trajectory as closely as possible, in the presence of various model uncertainties. The reference trajectory and its derivatives up to n^{th} order are assumed to be known, bounded, and piece-wise continuous.

3 Methodology

3.1 State Estimation

We assume only the output of the system is assumed to be measurable which means the full state of the system must be estimated. The parameterized Kreisselmeier observer has the advantage that the dynamics of the observer is completely separate from the parameters of the system [10]. This fact substantially simplifies the design of a suitable parameter adaptation scheme. The system given by Eqn. (1) can be rewritten in the following matrix form:

$$\dot{x} = A_o x + (K-a)x_1 + Bu + F\Lambda, \tag{3}$$

where

$$A_o = \begin{bmatrix} -k_n & 1 & 0 & \dots \\ \vdots & \vdots & \ddots & \vdots \\ -k_2 & 0 & \dots & 1 \\ -k_1 & 0 & \dots & 0 \end{bmatrix}, \quad K = \begin{bmatrix} k_n \\ \vdots \\ k_2 \\ k_1 \end{bmatrix},$$

$$a = \begin{bmatrix} a_{n-1} \\ \vdots \\ a_1 \\ a_0 \end{bmatrix}, \quad b = \begin{bmatrix} b_m \\ \vdots \\ b_1 \\ b_0 \end{bmatrix}, \quad d = \begin{bmatrix} d_l \\ \vdots \\ d_2 \\ d_1 \end{bmatrix},$$

$$B = \begin{bmatrix} 0_{(\rho-1)\times 1} \\ b \end{bmatrix}, \quad F = \begin{bmatrix} 0_{(n-l)\times 1} \\ d \end{bmatrix}.$$

Following the design procedure described in [9], the intermediate filter parameters are the solution of the following set of equations:

$$\begin{aligned} \dot{\xi}_n &= A_o \xi_n + K y(t), \qquad (4) \\ \dot{\xi}_i &= A_o \xi_i + e_{n-i} y(t), \quad 0 \le i \le n-1 \\ \dot{v}_j &= A_o v_j + e_{n-j} u(t), \quad 0 \le j \le m \\ \dot{\psi}_k &= A_o \psi_k + F q_k, \quad 0 \le k \le p \end{aligned}$$

where, e_{n-i} is the $(n-i)^{th}$ column of the $n \times n$ identity matrix. The estimated states are then computed as

$$\hat{x} = \xi_n - \sum_{i=0}^{n-1} a_i \xi_i + \sum_{j=0}^{m} b_j v_j + \sum_{k=0}^{p} \sigma_k \psi_k \tag{5}$$

with the estimation error, $\varepsilon_x = x - \hat{x}$, error dynamics given by

$$\dot{\varepsilon}_x = A_o \varepsilon_x + (a-K)\delta_y(t) + F\Delta. \tag{6}$$

By appropriately choosing the observer gain, K, the observer matrix, A_o, can be made Hurwitz resulting in a stable state estimator. The solution to Eqn. (6) can be divided into the zero input response, ε, which satisfies $\dot{\varepsilon} = A_o \varepsilon$, and the zero state response, ε_u. Given Assumption 3 and the fact that matrix A_o is chosen to be stable, we have $\varepsilon_u(t) \in \Omega_\varepsilon \triangleq \{\varepsilon_u(t) | \|\varepsilon_u(t)\| < \delta_u\}$ where $\delta_u(t)$ is known. In the controller design phase, we will combine ε_u, the observer error resulting from the zero state response, with the unstructured but bounded uncertainty, Δ. While ε, the initial state of the observer, will be treated as a disturbance and will be modulated by the robust control or feedback gain at each step of design.

3.2 Parameter Projection

The main drawback of the conventional adaptive controller is that the behavior of the parameter estimation and consequently the overall system performance are unknown when subject to unstructured uncertainties. Under Assumption 3, a discontinuous projection is utilized to solve the robustness problem of the parameter adaptation [2] such that

$$\dot{\hat{\Theta}} = Proj_{\hat{\Theta}}(\Gamma\tau) \tag{7}$$

where $\dot{\hat{\Theta}}$ and τ denote the estimated model parameters and the regressor respectively. We note that τ will be more clearly defined within the design procedure. This discontinuous projection guarantees the estimated parameters stay within the pre-defined bounded region given by:

$$\{\dot{\hat{\Theta}}\}_i = \begin{cases} 0 & \text{if } \hat{\theta}_i = \hat{\theta}_{i,max} \text{ and } \{\Gamma\tau\}_i > 0 \\ 0 & \text{if } \hat{\theta}_i = \hat{\theta}_{i,min} \text{ and } \{\Gamma\tau\}_i < 0 \\ \{\Gamma\tau\}_i & \text{otherwise} \end{cases}$$

This projection satisfy the property $\hat{\Theta}^T\left(\Gamma^{-1}Proj_{\hat{\Theta}}(\Gamma\tau)-\tau\right)\leq 0$ which will prove to be useful in our stability analysis [2].

3.3 Controller Design Procedure

We present a systematic algorithm based on the backstepping procedure to design a dynamic ARC (D-ARC) output tracking controller. The first two steps of the backstepping procedure are different from the rest due to the existing unknown high frequency gain b_m. The other steps up to the step when the actual input appears for the first time in the equations, *e.g.*, step ρ, are trivial and similar to the conventional ARC backstepping procedure [4, 9]. After ρ, the control input, u, appears in the design procedure. A conventional backstepping control design stops here and extracts the control signal and constructs the stabilizing Lyapunov function. The Lyapunov function is only a function of the states up to that stage while the other states are treated as stable since the internal dynamics of the system is stable. However, we move beyond the procedure in [5] and provide a procedure that is able to impact the components of the system dynamics not captured in previous procedures.

It is well known that the open loop system must be minimum phase to be stabilizable using a backstepping method. While we do *not* relax this requirement, our modeling of the uncertainties can be more effective in improving ARC performance. Unlike traditional backstepping, our procedure continues after encountering the control input where the control inputs' derivatives appear in the virtual input parameter designed in the subsequent steps. The approach enables us to shape the dynamics of the control input which allows us to filter out the high frequency chattering of the input. The inclusion of the input variable in the Lyapunov function will have the added benefit of limiting the control effort needed to decrease the steady state error. We briefly summarize this procedure below.

Step 1: The backstepping procedure starts by the derivation of the dynamics of the first error parameter, the output tracking error denoted as $z_1=y(t)-y_r(t)$ given by:

$$\dot{z}_1=x_2-a_{n-1}(y-\delta_y(t))+\dot{\delta}_y(t)-\dot{y}_r(t). \tag{8}$$

Since x_2 is not measurable, we replace it with its estimate given by the observer defined by Eqn. (3) resulting in:

$$x_2=\xi_{n,2}-\xi_{(2)}a+v_{(2)}b+\psi_{(2)}\Sigma+\varepsilon_{x_2} \tag{9}$$

where, ε_{x_2}, the estimation error of x_2, $v_{(2)}$, and $\psi_{(2)}$ defined as

$$\begin{aligned}\xi_{(2)} &\triangleq [\,\xi_{n-1,2},\xi_{n-2,2},\ldots,\xi_{0,2}\,],\\ v_{(2)} &\triangleq [\,v_{m,2},v_{m-1,2},\ldots,v_{0,2}\,],\\ \psi_{(2)} &\triangleq [\,\psi_{p,2},\psi_{p-1,2},\ldots,\psi_{1,2}\,].\end{aligned}$$

The notation $*_{ij}$ denotes the j-th element of the vector $*_i$. Substituting for x_2 in Eqn. (9) and using its estimate given by Eqn. (8), we can obtain the following expression for the dynamics of the first error parameter:

$$\dot{z}_1=b_m v_{m,2}+\xi_{n,2}+\Theta^T\bar{\omega}-\dot{y}_r(t)+\hat{\Delta}_1+\varepsilon_2. \tag{10}$$

where $\bar{\omega}=\omega-e_{n+1}^T v_{m,2}$, $\omega^T\triangleq[\,\xi_{(2)}^T,v_{(2)}^T,\psi_{(2)}^T\,]+e_1^T y$ is used to reconstruct the regressor, and $\hat{\Delta}_1=a_{n-1}\delta_y(t)+\dot{\delta}_y(t)+\varepsilon_u$ lumps all the bounded unstructured uncertainties to be dealt at the robust control design stage. We note e_i denotes the i^{th} column of the identity matrix of the proper size with $v_{m,2}$ being the obvious choice of the virtual input at this design stage since it is the actual control, $u(t)$, which appears only after differentiating the input ρ times (this is less than any other parameters in the equation, see Eqn. (5)).

If $v_{m,2}$ was is actual control, we can design a control law α_1 to stabilize the system given by Eqn. (10). Since it is not, we define z_2 as the error between actual and desired value of $v_{m,2}$, *i.e.*, $z_2\triangleq v_{m,2}-\alpha_1$. Now, considering α_1 as the new control input, we design the ARC to drive z_1 to be as small as possible despite the various system uncertainties. According to the ARC backstepping procedure the controller design is separated into two parts, $\alpha_1=\alpha_{1a}+\alpha_{1s}$. The first term is the adaptive part and is designed to compensate the parameter uncertainties, and the second term guarantees the robust stability of the system in the presence of unstructured uncertain dynamics.

Let $\varphi\triangleq\xi_{n,2}+\hat{\Theta}^T\bar{\omega}-\dot{y}_r(t)$ be the error dynamics, then Eqn. (10) can be rewritten as $\dot{z}_1=b_m z_2+b_m(\alpha_{1a}+\frac{1}{\hat{b}_m}\varphi)+b_m\left(\frac{1}{b_m}-\frac{1}{\hat{b}_m}\right)\varphi+b_m(\alpha_{1s,1}+\alpha_{1s,2})+\tilde{\Theta}^T\bar{\omega}+\hat{\Delta}+\varepsilon_2$ where $\tilde{\Theta}=\Theta-\hat{\Theta}$ denotes the parameter estimation error. In order to design the stabilizing control action, we propose the first Lyapunov function $V_1=\frac{1}{2}z_1^2+\frac{1}{q_1}\varepsilon^T P_o\varepsilon$. The positive definite matrix, P_o, is the solution of the Lyapunov equation for the observer, $A_o^T P_o+P_o A_o=-I$, and q_1 is a design parameter to be chosen. Then $\alpha_{1a}=-\frac{1}{\hat{b}_m}\varphi$ and $\alpha_{1s1}=-\frac{1}{b_{m,min}}(c_1 z_1+q_1 z_1)$ are chosen to stabilize V_1. Substituting them into $\dot{V}_1$ we get $\dot{V}_1\leq b_m z_1 z_2-c_1 z_1^2+z_1\{b_m\alpha_{1s2}+\tilde{\Theta}^T\phi_1+\Delta_1\}-q_1(z_1-1/2q_1\varepsilon_2)^2$.

To keep track of the procedure, new parameters are numbered as, $\phi_1\triangleq\bar{\omega}-\frac{1}{\hat{b}}\varphi e_{n+1}$, *and* $\Delta_1\triangleq\hat{\Delta}$. There exists a robust control function α_{1s2} satisfying the following conditions:

1. $z_1\{b_m\alpha_{1s2}+\tilde{\Theta}^T\phi_1+\Delta_1\}<r_1$, and
2. $\alpha_{1s2}z_1\leq 0$.

Examples of smooth α_{1s2} satisfying these two conditions can be found in [2] and [11]. Essentially, the first condition indicates that the synthesized robust controller dominates the model uncertainties. r_1 is a design parameter and the level of control accuracy is to be adjusted by this design parameter. Smaller r_1 leads to faster convergence, but also bigger control effort. The second condition ensures that α_{1s2} is dissipative in nature and does not interfere with the functionality of the adaptive control part α_{1a}.

Step 2: In the dynamics of the second error variable, $\dot{z}_2=\dot{v}_{m,2}-\dot{\alpha}_1$, the derivative of α_1 inherits uncertainties from the dynamics of the system. The uncertain part of it, $\dot{\alpha}_{1u}$, captures the uncertain parameters' estimation errors, structural uncertainties, and state estimation errors. The remaining known states and parameters can be lumped into $\dot{\alpha}_{1c}$which is defined as:

$$\begin{aligned}\dot{\alpha}_{1c} \triangleq\ & \frac{\partial\alpha_1}{\partial y}\left(\xi_{n,2}+\hat{\theta}^T\omega\right)+\frac{\partial\alpha_1}{\partial\xi_{n,2}}\left(-k_2\xi_{n,1}+k_2y(t)\right)\\ &+\frac{\partial\alpha_1}{\partial\xi_{(2)}}\dot{\xi}_{(2)}+\sum_{i=1}^{m}\frac{\partial\alpha_1}{\partial v_{i,2}}\left[A_o v_i+e_{n-i}u(t)\right]_2\\ &+\frac{\partial\alpha_1}{\partial\psi_{(2)}}\dot{\psi}_{(2)}+\frac{\partial\alpha_1}{\partial y_r}\dot{y}_r+\frac{\partial\alpha_1}{\partial\dot{y}_r}\ddot{y}_r,\\ \dot{\alpha}_{1u} \triangleq\ & \frac{\partial\alpha_1}{\partial y}\left(\tilde{\theta}^T\omega+\Delta_1+\varepsilon_2\right)+\frac{\partial\alpha_1}{\partial\hat{\theta}}\dot{\hat{\theta}}.\end{aligned}$$

The unknown part which cannot be worked out due to the various uncertainties must be dealt with via robust feedback. The known part can be easily compensated to shape the dynamics of the error. Therefore the second error subsystem is given by:

$$\dot{z}_2=\dot{v}_{m,2}-\dot{\alpha}_1=-k_2v_{m,1}+v_{m,3}-\dot{\alpha}_{1c}-\dot{\alpha}_{1u}. \quad (11)$$

Let the second Lyapunov function be defined as $V_2=V_1+\frac{1}{2}z_2^2+\frac{1}{q_2}\varepsilon^TP_o\varepsilon$. Like the first step, to stabilize the system $v_{m,3}$ is taken as the virtual input and $\alpha_2=\alpha_{2a}+\alpha_{2s}$ is the control designed to stabilize this subsystem with α_{2a} given by:

$$\alpha_{2a} \triangleq -\hat{b}_mz_1+k_2v_{m,1}+\dot{\alpha}_{1c}-c_2z_2-q_2\left(\frac{\partial\alpha_1}{\partial y}\right)^2z_2. \quad (12)$$

Substituting Eqn. (12) into Eqn. (11), the time derivative of the second Lyapunov function satisfies the following inequality:

$$\begin{aligned}\dot{V}_2\le\ & z_3z_2-c_1z_1^2-c_2z_2^2+z_1\left\{b_m\alpha_{1s2}+\tilde{\theta}^T\phi_1+\Delta_1\right\}\\ &+z_2\left\{\alpha_{2s}+\tilde{\theta}^T\phi_2+\Delta_2\right\}-z_2\frac{\partial\alpha_1}{\partial\hat{\theta}}\dot{\hat{\theta}}\\ &-q_1\left(z_1-\frac{1}{2q_1}\varepsilon_2\right)^2-q_2\left(z_2\left(\frac{\partial\alpha_1}{\partial y}\right)+\frac{1}{2q_2}\varepsilon_2\right)^2\end{aligned}$$

with $\phi_2 \triangleq -\left(\frac{\partial\alpha_1}{\partial y}\right)\omega+e^*_{n+m+1}z_1$ and $\Delta_2 \triangleq -\left(\frac{\partial\alpha_1}{\partial y}\right)\hat{\Delta}$. The above equation tells us if $v_{m,2}$ is our input, we can stability the subsystem by choosing the control signals to satisfy given conditions. However, since we do not access to the actual control input yet, we continue the procedure.

Step j $(3\le j\le(\rho-1))$: By mathematical induction the results for all intermediate steps up to $\rho-1$ can be proven. For step j we express the derivative of $z_j=v_{m,j}-\alpha_{j-1}$ as $\dot{z}_j=-k_jv_{m,1}+v_{m,j+1}-\dot{\alpha}_{(j-1)c}-\dot{\alpha}_{(j-1)u}$. Similar to previous steps, $\dot{\alpha}_{(j-1)c}$ encapsulates all the known terms with $\dot{\alpha}_{(j-1)u}$ containing the unknown terms. Treating $v_{m,(j+1)}$ as the virtual control input, the compensation part is synthesized similar to Eqn. (12): $\alpha_{ja} \triangleq -z_{(j-1)}+k_jv_{m,1}+\dot{\alpha}_{j-1c}-c_jz_j-q_j\left(\frac{\partial\alpha_{j-1}}{\partial y}\right)^2z_j$. The j^{th} *Lyapanov* function would be defined as $V_j=V_{j-1}+\frac{1}{2}z_j^2+\frac{1}{q_j}\varepsilon^TP_0\varepsilon$ and its time derivative given by

$$\begin{aligned}\dot{V}_j\le\ & z_jz_{(j+1)}-\sum_{i=1}^{j}c_iz_i^2-\left(\sum_{i=2}^{j}z_i\frac{\partial\alpha_{i-1}}{\partial\hat{\theta}}\right)\dot{\hat{\theta}}\\ &+z_1\left\{b_m\alpha_{1s2}+\tilde{\theta}^T\phi_1+\Delta_1\right\}+\sum_{i=2}^{j}z_i\left\{\alpha_{is}+\tilde{\theta}^T\phi_i+\Delta_i\right\}\\ &-q_1\left(z_1-\frac{1}{2q_1}\varepsilon_2\right)^2-\sum_{i=2}^{j}q_i\left(z_i\left(\frac{\partial\alpha_{i-1}}{\partial y}\right)+\frac{1}{2q_i}\varepsilon_2\right)^2\end{aligned}$$

Step ρ: This is the step where the actual control input, $u(t)$, appears in the design procedure for the first time as a part of $\dot{v}_{m,\rho}$. The conventional procedure ends the backstepping at this step and extracts control input. However, in our method we continue with the procedure and define $z_\rho=v_{m,\rho}-\alpha_{\rho-1}$ such that $\dot{z}_\rho=-k_\rho v_{m,1}+v_{m,(\rho+1)}+u-\dot{\alpha}_{(\rho-1)c}-\dot{\alpha}_{(\rho-1)u}$. Then $\alpha_{\rho a}$ is synthesized the same way as α_{ja} as in Step j, except that it is augmented by u resulting in $\alpha_{\rho a} \triangleq -z_{(\rho-1)}+k_\rho v_{m,1}-u+\dot{\alpha}_{(\rho-1)c}-c_\rho z_\rho-q_\rho\left(\partial\alpha_{(\rho-1)}/\partial y\right)^2z_\rho$.

Step k $((\rho+1)\le k\le(n-1))$: The significance of these steps with respect to step ρ and consequently the steps before is that the time derivatives of the control input, $u(t)$, now appears in the equations as part of $\dot{\alpha}_{(k-1)c}$ as seen below:

$$\begin{aligned}\dot{\alpha}_{(k-1)c} \triangleq\ & \frac{\partial\alpha_{k-1}}{\partial y}\left(\xi_{n,2}+\hat{\theta}^T\omega\right)+\sum_{i=2}^{k-1}\frac{\partial\alpha_1}{\partial\xi_{(i)}}\dot{\xi}_{(i)} \quad (13)\\ &+\sum_{i=2}^{l}\frac{\partial\alpha_{k-1}}{\partial\psi_{(i)}}\dot{\psi}_{(i)}+\sum_{j=2}^{k-1}\sum_{i=1}^{m}\frac{\partial\alpha_{k-1}}{\partial v_{i,j}}\left(\dot{v}_i\right)_j\\ &+\sum_{i=1}^{k-1-\rho}\frac{\partial\alpha_{k-1}}{\partial u^{(i-1)}}u^{(i)}+\sum_{i=1}^{k-1}\frac{\partial\alpha_{k-1}}{\partial y_r^{(i-1)}}y_r^{(i)}.\end{aligned}$$

Step n: In this final step the D-ARC output tracking controller is synthesized. As in the previous steps, we express the derivative of z_n as $\dot{z}_n=\dot{v}_{m,n}-\dot{\alpha}_{(n-1)}=-k_nv_{m,1}-\dot{\alpha}_{(n-1)c}-\dot{\alpha}_{(n-1)u}$. The unknown and known parts of $\dot{\alpha}_{(n-1)}$ are not so different from their counterparts in the previous steps. In this step we note that $v_{m,j}$, which has been treated as a virtual input, no longer appears in the error dynamics. To stabilize the Lyapanov function, suitable dynamics is imposed on this error subsystem by holding the following for the n^{th} error dynamics:

$$\begin{aligned}k_nv_{m,1}+\dot{\alpha}_{(n-1)c}=\ & c_nz_n+z_{n-1} \quad (14)\\ &-\alpha_{sn}+q_n\left(\frac{\partial\alpha_{(n-1)}}{\partial y}\right)^2z_n.\end{aligned}$$

Then, the time derivative of the overall Lyapunov function,

$V = V_n = \frac{1}{2}\sum_{i=1}^{n} z_i^2 + \sum_{i=1}^{n} \frac{1}{q_i}\varepsilon^T P_0 \varepsilon$, satisfies:

$$\dot{V}_n \leq -\sum_{i=1}^{n} c_i z_i^2 + z_1\left\{b_m \alpha_{1s2} + \tilde{\theta}^T\phi_1 + \Delta_1\right\} + \sum_{i=2}^{n} z_i\left\{\alpha_{is} + \tilde{\theta}^T\phi_i + \Delta_i\right\} + \left(\sum_{i=2}^{n} z_i \frac{\partial \alpha_{(i-1)}}{\partial \hat{\theta}}\right)\dot{\hat{\theta}}. \quad (15)$$

The control input u is then obtained by solving the linear time-varying differential Eqns. (13) and (14) resulting in:

$$\begin{aligned} u^{(m)} = & \frac{1}{\frac{\partial \alpha_{(n-1)}}{\partial u^{(m-1)}}}\Bigg\{ -k_n v_{m,1} + c_n z_n + q_n\left(\frac{\partial \alpha_{(\rho-1)}}{\partial y}\right)^2 z_n \quad (16) \\ & - \sum_{i=2}^{(n-1)} \frac{\partial \alpha_{n-1}}{\partial \xi_{(i)}}\dot{\xi}_{(i)} - \frac{\partial \alpha_{(k-1)}}{\partial y}\left(\xi_{n,2} + \hat{\theta}^T\omega\right) \\ & - \sum_{i=2}^{l} \frac{\partial \alpha_{n-1}}{\partial \psi_{(i)}}\dot{\psi}_{(i)} - \sum_{j=2}^{n}\sum_{i=1}^{m} \frac{\partial \alpha_{n-1}}{\partial v_{i,j}}(\dot{v}_i)_j \\ & - \left(\sum_{i=2}^{(n)} z_i \frac{\partial \alpha_{(i-1)}}{\partial \hat{\theta}}\right)\phi_n - \alpha_{sn} - \sum_{i=1}^{k-\rho-1} \frac{\partial \alpha_{(k-1)}}{\partial u^{(i-1)}} u^{(i-1)} \Bigg\}. \end{aligned}$$

3.4 Stability Analysis

The Lyapunov function defined in the previous section embeds the states of the n-dimensional plant given by Eqn. (2), the three n-dimensional filters given by Eqn. (4), and the $n+m+p+2$ estimated parameters. The rest of the states can be proven to be stable since the estimation filter is stable and the system is minimum phase [9].

Lemma 1. *Let the parameter estimate be updated by Eqn.* (7) *with* $\tau = \sum_{i=2}^{n} z_i\phi_i$, $\phi_i \overset{def}{=} -\left(\partial\alpha_{(i-1)}/\partial y\right)\bar{\omega}$ *with* $i = 1,\cdot,n$, *and* $\phi_1 \overset{def}{=} \bar{\omega} + \frac{1}{b}\varphi e_{n+1}$, $\phi_2 \overset{def}{=} -\left(\frac{\partial\alpha_1}{\partial y}\right)\bar{\omega} + e^*_{n+1} z_1$. *If the control parameters,* c_i, *are chosen such that* $c_i = f_i + g_i\|\Gamma\phi_i\|^2 + h_i\left\|\frac{\partial\alpha_{(i-1)}}{\partial\hat{\theta}}\right\|^2$, *where* $f_i, g_i, h_i > 0$ *are chosen such that* $g_i \geq \frac{n}{4}\sum_{j=1}^{n}\frac{1}{h_j}$, *then the system is stable with respect to the Lyapanov function* V, *and the control law* u *guarantees that*

$$V \leq \exp(-2f_v t)V(0) + \frac{r_v}{2f_v}\left[1 - \exp(-2f_v t)\right] \quad (17)$$

where $f_v \overset{\Delta}{=} min(f_1, f_2, , f_n)$ *and* $r_v \overset{\Delta}{=} \sum_{j=1}^{n} r_j$.

Proof. Noting that $\left\|\dot{\hat{\theta}}\right\|^2 = \left\|Proj_{\hat{\theta}}(\Gamma\tau)\right\|^2 \leq \|\Gamma\tau\|^2$, and according to the triangular inequality, $\left\|\dot{\hat{\theta}}\right\|^2 \leq n\sum_{j=1}^{n}\left\|\Gamma\phi_j\right\|^2 z_j^2$. For any positive number of h_i, the inequality

$$\left|\sum_{i=1}^{n} z_i \frac{\partial\alpha_{(i-1)}}{\partial\hat{\theta}}\dot{\hat{\theta}}\right| \leq \sum_{i=1}^{n}\left(h_i\left\|\frac{\partial\alpha_{(i-1)}}{\partial\hat{\theta}}\right\|^2 z_i^2 + \frac{1}{4h_i}\left\|\dot{\hat{\theta}}\right\|^2\right)$$

results from the expansion of a quadratic equation. By choosing g_i and h_i as above and considering the upper bound of the adaptive parameters in Eqn. (17), we have

$$\left|\sum_{i=1}^{n} z_i \frac{\partial\alpha_{(i-1)}}{\partial\hat{\theta}}\dot{\hat{\theta}}\right| \leq \sum_{i=1}^{n} h_i\left\|\frac{\partial\alpha_{(i-1)}}{\partial\hat{\theta}}\right\|^2 z_i^2 + \sum_{j=1}^{n} g_i\left\|\Gamma\phi_j\right\|^2 z_j^2.$$

Then, $\dot{V}_n \leq -\sum_{i=1}^{n} f_i z_i^2 + \sum_{i=1}^{n} r_i$, which results in the bound given by Eqn. (17).

The same result as in [2,4] holds for the stability of the parameter adapive mechanism and the tracking performance of the system. For the sake of completeness, we present the equivalent theorem to that in [2,4].

Theorem 1. *Given the desired output trajectory* $y_d(t)$ *generated described in [2], if the control input is designed as in Eqn.* (16)*, and using the parameter update law given by Eqn.* (7)*, the following results hold:*

(A) All signals are bounded and the output tracking error is guaranteed to have any desired transient performance.
(B) If the dynamic uncertainties vanish after a finite time, in the presence of only parametric uncertainties, asymptotic output tracking is guaranteed for any control gains.

4 Simulation

The proposed method is applied to the design of an adaptive robust feedback controller for a voice coil motor (VCM) which is used in various precision applications. A well-known use of VCM is as an actuator for the read/write head of a computer hard disk drive (HDD) [8,12]. The system operates in two modes: "track following" and "track seeking". The read/write head must achieve precise positioning on a desired track in the track following mode or transition quickly from one track to another in the track seeking mode. Switching control and multi-rate control are often used to accomplish both tasks [13,14]. However, the ARC provides an approach a single unifying control strategy for this application since it has shown promising results for each single-stage and dual-stage hard disk servo systems [11,15].

The model given for the VCM actuator consists of nonlinear coefficients of viscous and coulomb friction, and the nonlinear effects of the hysteresis loop [16] [17] [18]. In order to apply linear robust control to this problem, the actuator must be represented as a linear model with matched uncertainty. This idea is used extensively in many applications, where linear H_∞ or $\mu-synthesis$ schemes are used to design the controller. Examples of linear models for VCM actuators can be found in [12,19]. To be able to compare the results of this paper with existing methods, the model used here is the one presented in these references. We refer the interested reader to [12,19] for the details on how the models were derived experimentally. The transfer function relating the input voltage U_v to the tip displacement Y_v is given by:

$$G_v(S) = \sum_{i=0}^{6}\frac{A_i}{S^2 + 2\xi_i\omega_i S + \omega_i^2}$$

Table 1. Poles and Zeros of the nominal system identified for the VCM

Poles	Zeros	
$(-0.0230 \pm j0.0896) \times 10^4$	$(-0.0076 \pm j0.1317) \times 10^4$	
$(-0.0089 \pm j0.1295) \times 10^4$	$(-0.0214 \pm j0.1333) \times 10^4$	
$(-0.0124 \pm j0.1401) \times 10^4$	$(-0.0898 \pm j1.9927) \times 10^4$	
$(-0.0915 \pm j1.8589) \times 10^4$	$(-0.0770 \pm j3.5620) \times 10^4$	
$(-0.0729 \pm j3.1183) \times 10^4$	$(2.4248 \pm j7.3828) \times 10^4$	
$(-0.0747 \pm j6.6933) \times 10^4$	2.5886×10^4	-5.5608×10^4

Table 2. Joint observability and controllability Gramians of the nominal model of VCM

Modes	Grammians	Modes	Grammians
1	**123.74**	7	0.57
2	**73.96**	8	0.56
3	**12.55**	9	0.33
4	**10.77**	10	0.33
5	3.74	11	0.25
6	3.31	12	0.23

where for each mode i, A_i is the modal constant, ξ_i is the damping ratio, and ω_i is the natural frequency.

The nominal model extracted from the system identification data is order 12 with relative degree of 2. A VCM is intrinsically a minimum phase system. However, when the sensor and actuator are none-collocated the flexibility of the arm contributes a limiting non-minimum phase zero into the overall transfer function [7] [8]. These non-minimum phase zeros become the unstable internal modes of the system during the backstepping procedure, and destabilize the observer, the controller, and consequently the whole closed-loop system. The strategy then is to reduce the order of the nominal model so such undesirable high frequency characteristics of the model is lumped with other uncertainties of the system and rejected by the robust part of the ARC.

4.1 Model Order Reduction

The implementation of a dynamic backstepping controller for a high order system requires high computational cost. As such, it makes sense to reduce the order of the model of the system. In general, a high order system model can be replaced by lower order approximation without a noticeable difference in the model resolution. To achieve this model reduction, we note that a dynamic component of a linear system corresponding to a low value of the joint observability and controllability Gramians can be safely eliminated from the overall dynamic equation with minimum effect on the input-output behavior of the model [20]. Table 2 shows the joint observability and controllability Gramians of the balanced realization of the nominal model of the VCM. Table 2 shows two groups of modes: modes 1-6 and 7-12 for which the joint Gramians are respectively greater than and less than one. Further, the Gramians of modes 5 and 6 are less than one third of the Gramians of the mode 4. Thus, we conclude that the dynamic behavior of the nominal VCM model is dominated by first four modes with greatest Gramians.

The Bode plot of the high order nominal system and the reduced model is presented in Fig. 2. The reduced model is of the 4^{th} order and is obtained using a Hankel Norm Order Reduction. The reduced order system has the relative degree of one, which means the conventional ARC design procedure would be made up of one step. As such, we expect considerable performance improvement when the proposed dynamic adaptive robust backstepping method is applied.

Table 3. Poles and Zeros of the reduced nominal model

Poles	Zeros
$(-0.0254 \pm j0.0908) \times 10^4$	-5.1010×10^4
$(-0.0086 \pm j0.1481) \times 10^4$	$(-0.0129 \pm j0.9083) \times 10^4$

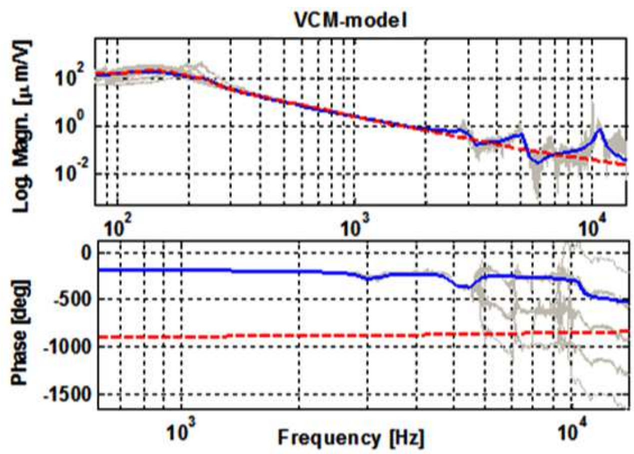

Fig. 2. The frequency response estimates of VCM system given by Eqn. (18) including Voltage-to-Current converter (dotted), high order nominal model (solid), and the reduced model (dashed). The figure was produced using data provided by [12, 19].

4.2 Control Design

The reference trajectory is generated using the structural vibration minimized acceleration trajectory (SMART) procedure described in [21]. The idea is to solve the optimal trajectory planing problem with $J = \int_{t_0}^{t_f} \left[\frac{du_{SMART}}{dt}\right]^2 dt$ as the cost function for a double integrator plant. The solution to this problem can be analytically obtained, with the optimal reference trajectory given by:

$$
\begin{aligned}
y_{ref,SMART}(t) = & \left(6y_f - 3v_f t_f + \frac{a_f}{2} t_f^2\right)\left(\frac{t}{t_f}\right)^5 \\
& + \left(-15y_f + 7v_f t_f - a_f t_f^2\right)\left(\frac{t}{t_f}\right)^4 \\
& + \left(10y_f - 4v_f t_f + \frac{a_f}{2} t_f^2\right)\left(\frac{t}{t_f}\right)^3
\end{aligned}
$$

Table 4. The parameters of the Dynamic Adaptive Robust Controller designed for the VCM

$c_1 = 5\times 10^3 + 10^{-16}\|\Gamma\phi_1\|^2$ $c_2 = 10^3 + 10^{-17}\|\Gamma\phi_2\|^2 + 10^3\left\|\frac{\partial\alpha_1}{\partial\hat{\theta}}\right\|^2$	$d_1 = 10^2,\ r_1 = 10$ $d_2 = 10^{-3},\ r_2 = 10$
$\varepsilon_{u1} = 10$ $\varepsilon_{u2} = \left\|\frac{\hat{\theta}(1)}{\hat{\theta}(5)} - \frac{(c_1+d_1)}{\hat{\theta}(5)}\right\|.\varepsilon_{u1}$	$h_1 = 10.\|\phi_1\| + \varepsilon_{u1}$ $h_2 = 10.\|\phi_2\| + \varepsilon_{u2}$
$\Gamma = diag([5\times 10^2; 5\times 10^8; 10^{11}; 10^{12}; 10^3; 10^9; 5\times 10^{14}; 10^{18}])$	

Table 5. The simulation results and performance indices

Performance Index	Set 1	Worse Case
$e_M(\mu m)$	2.41	3.12
$\mathscr{L}_2[e]\,(\mu m)$	1.82	2.32
$\mathscr{L}_2[u]\,(volt)$	24.65	28.39

where t_f is the rise time, and v_f and a_f are the first and second derivatives of the reference position trajectory. The designed trajectory is to receive track number 648 with each track's width equal to $3.945\mu m$. The track seeking time is 5 *msec*.

The model simplifications and reductions taken results in nontrivial model parameter uncertainties and unmodeled dynamics. If the conventional backstepping scheme is used to design the ARC, the dynamic uncertainties would have to be lumped into one Δ to be dealt with at the first step when the actual input variable appears in the equations. Such a controller can not possibly stabilize this system. However, using the D-ARC, the backstepping can advance into the dynamics of the system where the lumped uncertainty branches out to the various channels of the system. The robust part of the controller can then reject their effects and stabilize the system.

To compare our simulation results with existing controllers presented in the literature, the following performance metrics are used: 1) the average tracking performance index, $\mathscr{L}_2[e]$, 2) the maximum absolute value of the tracking error, e_M, and, 3) the mean value of the control input, $\mathscr{L}_2[u]$. These metrics were chosen to evaluate the performance of the system in the track seeking and following modes and the average control input. Table 5 summarizes these performance indicators for a typical and a worse case scenario among the simulations for the various samples of uncertain system model.

Figure 4 shows the performance of the controller in a run for a sample model of the uncertain system. These results show the smoothness of the control signal and improved performance of the system for the transient and steady state behaviors. Figure 5 shows how the model parameters adapt over time. Parameter adaptation enables the system to reduce model uncertainty resulting in a accurate system model and more precise tracking performance with much less control effort.

The main source of external disturbances to the head positioning servo system is the rotation of the spindle motor. Other significant disturbances include vibration shocks, mechanical disturbances like disk fluttering and slider vibration, and electrical noise. The disturbances of the HDD servo design problem are lumped together as an output disturbance and is known as *runouts* [22]. The disturbance rejection capability of the proposed controller is tested by injecting a simulated runout signal given by $w(t) = 0.5 + 0.1cos(110\pi t) + 0.05sin(220\pi t) + 0.02sin(440\pi t) + 0.01sin(880\pi t)\ \mu m$. The signal was applied at $t = 0.01\ s$ after the output has reached steady state. Figure 4b shows the controller rejecting the runout in less than 5 *ms*. The oscillations are due to the nature of the sliding mode control. While these oscillations are higher frequency than previous proposed methods, they have significantly less energy and would most likely be damped out by the rigidity of the head and should not dislocate the head from the target track.

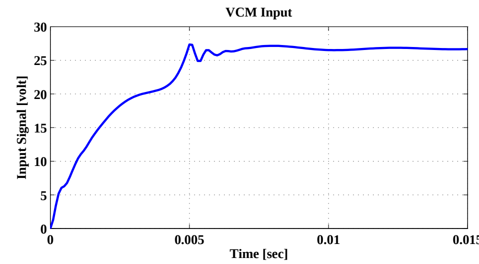

(a) VCM Input Voltage

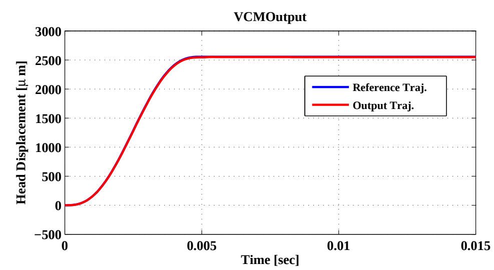

(b) VCM Tracking Performance

Fig. 3. Tracking Performance of VCM controlled with first order Dynamic ARC

5 Conclusion

We presented an alternative dynamic backstepping algorithm to synthesize a dynamic adaptive robust controller (D-ARC). The proposed method addresses the inherent weakness in the way uncertainties are modeled in the conventional ARC backstepping approach to improve the stability and performance of the system. Simulations for a VCM actuator shows that the proposed method is more effective than

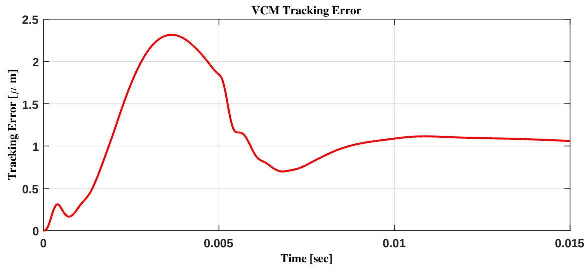

(a) Tracking Error of VCM controlled with first order Dynamic ARC

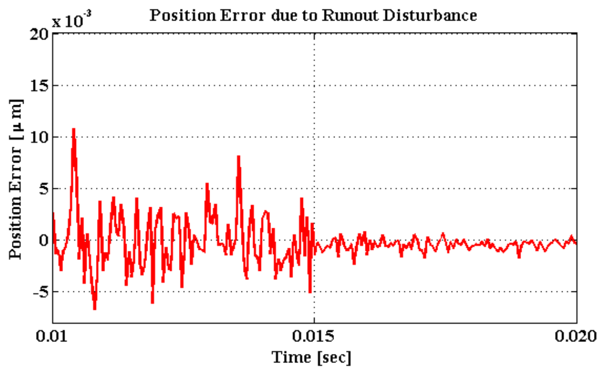

(b) Runout error due to the output disturbance

Fig. 4. Tracking Error of VCM controlled with first order Dynamic ARC

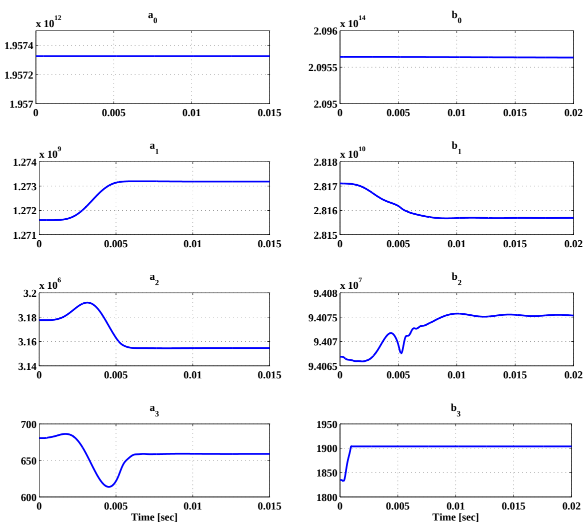

Fig. 5. Adaptation parameter variation in track-seeking/track-flowing mode

a static control strategy since the DARC signal is smoother and results in a significantly improved the transient performance of the system.

In general, one would expect a high precision and agile system such as the VCM to exhibit high frequency oscillations regardless of how smooth the switching function is in the control input. However, there is no sign of oscillations in either the control signal or the tracking error of the control system suggesting that these high frequencies are filtered out since the procedure accounts for the dynamics of the control effort as seen in Fig. 3. How to further shape the dynamics of the control input is a direction for future work. Figure 5 show better estimate of the model parameters leads to improved system performance.

We note that the model order reduction of the VCM resulted in a fourth order system. This suggests the the non-minimum phase dynamics of the system was transferred into the parts of the model that describes the uncertainties of the system. In [23], zero placement was performed before the ARC was designed using an equivalent minimum-phase system. Using similar performance metrics to compare the results of our approach with those in [23] (see Table III in [23]) suggests that our method significantly improves the transient performance of the system. In [24], an optimal nonlinear gain tuning method was applied to the design of a composite nonlinear feedback controller for a VCM in an HDD servo system. The method achieved track seeking and track following errors of $\pm 20\mu m$ which is almost ten times worst than our results. A more recent paper introduced an enhancement to the adaptive robust controller design [25]. In [25], a μ-synthesis robust feedback controller was used to deal with the unstructured uncertainty of the system and an adaptive feedforward compensation was used to estimate the uncertain parameters of the model. While the strategy showed promising steady state performance, the strategy does little to ameliorate the system's transient response since the transient response is mostly impacted by the unstructured uncertainties. As such, the proposed DARC strategy outperforms the mentioned existing approaches.

References

[1] Ikhouane, F., and Krstic, M., 1998. "Robustness of the tuning functions adaptive backstepping design for linear systems". *Automatic Control, IEEE Transactions on*, **43**(3), Mar, pp. 431–437.

[2] Yao, B., Al-Majed, M., and Tomizuka, M., 1997. "High-performance robust motion control of machine tools: an adaptive robust control approach and comparative experiments". *IEEE/ASME Transactions on Mechatronics*, **2**(2), June, pp. 63–76.

[3] Yao, B., and Jiang, C., 2010. "Advanced motion control: From classical pid to nonlinear adaptive robust control". In Advanced Motion Control, 2010 11th IEEE International Workshop on, pp. 815–829.

[4] Xu, L., and Yao, B., 1999. "Output feedback adaptive robust control of uncertain linear systems with large disturbances". In Proceedings of American Control Conference, Vol. 1, pp. 556–560 vol.1.

[5] Zinober, A., Scarratt, J., Mills, R., and Koshkouei, A., 2001. "New developments in dynamical adaptive backstepping control". Vol. 259 of *Lecture Notes in Control and Information Sciences*. Springer London, pp. 565–622.

[6] Herrmann, G., Turner, M., Postlethwaite, I., and

Guo, G., 2004. "Practical implementation of a novel anti-windup scheme in a hdd-dual-stage servo-system". *Mechatronics, IEEE/ASME Transactions on,* **9**(3), Sept, pp. 580–592.

[7] Wang, D. S., Yang, G.-B., and Donath, M., 1993. "Non-collocated flexible beam motion control based on a delayed adaptive inverse method". In American Control Conference, 1993, pp. 552–559.

[8] Rigney, B. P., Pao, L. Y., and Lawrence, D. A., 2010. "Nonminimum phase adaptive inverse control for settle performance applications". *Mechatronics,* **20**(1), pp. 35 – 44. Special Issue on Servo Control for Data Storage and Precision Systems, from 17th {IFAC} World Congress 2008.

[9] Krstic, M., Kokotovic, P. V., and Kanellakopoulos, I., 1995. *Nonlinear and Adaptive Control Design*, 1st ed. John Wiley & Sons, Inc., New York, NY, USA.

[10] Kreisselmeier, G., 1977. "Adaptive observers with exponential rate of convergence". *Automatic Control, IEEE Transactions on,* **22**(1), Feb, pp. 2–8.

[11] Taghirad, H., and Jamei, E., 2008. "Robust performance verification of adaptive robust controller for hard disk drives". *Industrial Electronics, IEEE Transactions on,* **55**(1), Jan, pp. 448–456.

[12] Herrmann, G., and Guo, G., 2004. "{HDD} dual-stage servo-controller design using a -analysis tool". *Control Engineering Practice,* **12**(3), pp. 241 – 251. Benchmarking Modelling and Control in Wastewater Treatment.

[13] Venkataramanan, V., Chen, B. M., Lee, T. H., and Guo, G., 2002. "A new approach to the design of mode switching control in hard disk drive servo systems". *Control Engineering Practice,* **10**(9), pp. 925 – 939.

[14] Huang, X., Nagamune, R., and Horowitz, R., 2006. "A comparison of multirate robust track-following control synthesis techniques for dual-stage and multisensing servo systems in hard disk drives". *Magnetics, IEEE Transactions on,* **42**(7), July, pp. 1896–1904.

[15] Zhong, J., and Yao, B., 2008. "Adaptive robust precision motion control of a piezoelectric positioning stage". *Control Systems Technology, IEEE Transactions on,* **16**(5), Sept, pp. 1039–1046.

[16] Ratliff, R., and Pagilla, P., 2005. "Design, modeling, and seek control of a voice-coil motor actuator with nonlinear magnetic bias". *Magnetics, IEEE Transactions on,* **41**(6), June, pp. 2180–2188.

[17] Peng, K., Chen, B., Cheng, G., and Lee, T., 2005. "Modeling and compensation of nonlinearities and friction in a micro hard disk drive servo system with nonlinear feedback control". *Control Systems Technology, IEEE Transactions on,* **13**(5), Sept, pp. 708–721.

[18] de Callafon, R., Nagamune, R., and Horowitz, R., 2006. "Robust dynamic modeling and control of dual-stage actuators". *Magnetics, IEEE Transactions on,* **42**(2), Feb, pp. 247–254.

[19] Taghirad, H., and Sheykholeslami, P., 2007. "Adaptive robust controller design for a dual-stage hard disk drive". In Advanced intelligent mechatronics, 2007 IEEE/ASME international conference on, pp. 1–6.

[20] Pernebo, L., and Silverman, L., 1982. "Model reduction via balanced state space representations". *Automatic Control, IEEE Transactions on,* **27**(2), Apr, pp. 382–387.

[21] Hara, S., Hara, T., Yi, L., and Tomizuka, M., 2000. "Novel reference signal generation for two-degree-of-freedom controllers for hard disk drives". *Mechatronics, IEEE/ASME Transactions on,* **5**(1), Mar, pp. 73–78.

[22] Graham, M., and de Callafon, R., 2006. "An iterative learning design for repeatable runout cancellation in disk drives". *Control Systems Technology, IEEE Transactions on,* **14**(3), May, pp. 474–482.

[23] Ataollahi, M., Eghrary, H., and Taghirad, H., 2011. "Adaptive robust backstepping control design for a non-minimum phase model of hard disk drives". In Electrical Engineering (ICEE), 2011 19th Iranian Conference on, pp. 1–1.

[24] Lan, W., Thum, C., and Chen, B., 2010. "A hard-disk-drive servo system design using composite nonlinear-feedback control with optimal nonlinear gain tuning methods". *Industrial Electronics, IEEE Transactions on,* **57**(5), May, pp. 1735–1745.

[25] Chen, Z., Yao, B., and Wang, Q., 2015. "μ -synthesis-based adaptive robust control of linear motor driven stages with high-frequency dynamics: A case study". *Mechatronics, IEEE/ASME Transactions on,* **20**(3), June, pp. 1482–1490.